ORIGINAL RESEARCH ARTICLE UHD JOURNAL OF SCIENCE AND TECHNOLOGY

A Boundary Integral Equation Method for Computing Numerical Conformal Mappings onto the Disk with Rectilinear Slit and Spiral Slits Regions

Ali W.K. Sangawi

Department of General Sciences, College of Education, Charmo University, 46023 Chamchamal, Sulaimani, Kurdistan, Iraq.

ABSTRACT

This article proposes a boundary integral equation method for computing numerical conformal mappings of bounded multiply connected region Ω onto the disk with rectilinear slit and spiral slits regions, Ω_1 and Ω_2 Initially, the process involves calculating the boundary value of the canonical region. Cauchy's integral formula can then be used to compute the mapping of the interior values. The effectiveness of the proposed method is demonstrated using several numerical examples.

Index Terms: Numerical conformal mapping, Boundary integral equations, multiply connected regions, Generalized Neumann kernel

1. INTRODUCTION

The identification of canonical regions plays a crucial role in conformal mappings of multiply connected regions. The regions identified as canonical include the disk with circular slits, the annulus with circular slits, the circular slit region, the radial slit region, and the parallel slit region. Furthermore, additional canonical regions for conformal mappings include the disk with spiral slits region, annulus with spiral slits region, spiral slits region, and straight slits region [1]-[13]. Nasser's method of computing conformal mapping is based on Riemann-Hilbert problem [2], [5], [14], while Sangawi's methods rely on integral equations satisfy the interior non-homogeneous boundary relationship [8]-[12].

Access this article online

DOI:10.21928/uhdjst.v7n1y2023.pp92-99	E-ISSN: 2521-4217 P-ISSN: 2521-4209

The canonical slit regions introduced by Koebe [1], DeLillo *et al.* [15], and Nasser [5] are special cases of the spiral slits region. Sangawi [9]-[11] and Sangawi *et al.* [12] have demonstrated conformal mapping of bounded multiply connected regions onto the second, third, and fourth categories of Koebe's canonical slit regions using a boundary integral equation method. In Nasser [14] study, the study of bounded multiply connected region onto the disk with rectilinear slit and spiral slits region was facilitated by reformulating the conformal mapping as a Riemann-Hilbert problem. The present paper aims to establish a new boundary integral equation method for numerical conformal mappings from Ω onto Ω_1 and Ω_2.

The design of the study is as follows: Section 2 presents some necessary materials. A derivation of integral equation method

Corresponding author's e-mail: Ali W.K. Sangawi, Department of General Sciences, College of Education, Charmo University, 46023 Chamchamal, Sulaimani, Kurdistan, Iraq. E-mail: ali.kareem@charmouniversity.org

Received: 02-04-2023 Accepted: 25-04-2023 Published: 10-06-2023

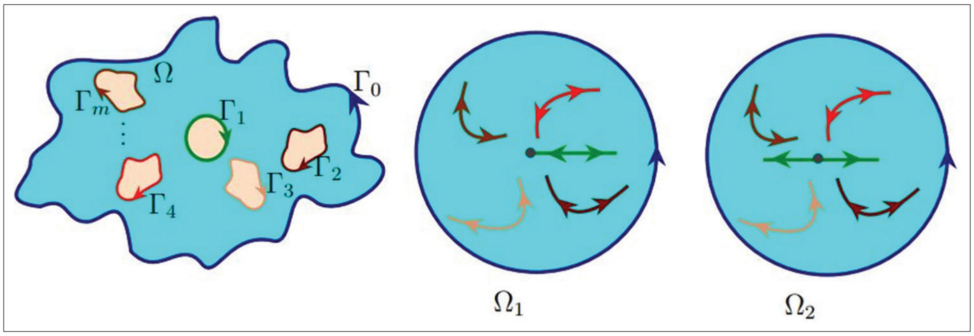

Fig. 1. Mapping of Ω onto Ω_1 and Ω_2.

for computing the function $\mathcal{F}$ has been presented in Section 3. The boundary integral equation method has been illustrated through examples provided in Section 4. Lastly, Section 5 comprises of the conclusion.

2. NECESSARY MATERIALS

A bounded multiply connected region **Ω** of connectivity M + 1. The boundary Γ consists of M + 1 smooth Jordan curves $\Gamma_\iota, \iota=0,1,\ldots,M$ as demonstrated in the following, (see Fig. 1)

The curve Γ_ι is parametrized by a 2π periodic twice continuously differentiable complex function $\xi_\iota(t)$

$$\zeta_\iota(t)=\frac{d\,\zeta_\iota(t)}{d\,t}\neq 0,\quad t\in_\iota=[0,2\pi],\quad \iota=0,\ldots,M$$

The complete parameter I is the combination of M + 1 disjoint intervals I_ι, $\iota = 0,\ldots,$M. The entire boundary Γ on I is defined by parametrization $\xi(t)$

$$\zeta(t)=\begin{cases}\zeta_0(t), & t\in I_0=[0,2\pi],\\ \zeta_1(t), & t\in I_1=[0,2\pi],\\ \quad\vdots & \\ \zeta_m(t), & t\in I_m=[0,2\pi]\end{cases}$$

Assuming $\hat{A}(t)$ is a complex function that is continuously differentiable with a periodicity of 2π $\forall t\in I_\iota$. The generalized Neumann kernel that is formed using $\hat{A}$ can be described as[16]:

$$\hat{N}(t,s)=\begin{cases}\dfrac{1}{\pi}\operatorname{Im}\left(\dfrac{\hat{A}(t)}{\hat{A}(s)}\dfrac{\zeta'(s)}{\zeta(s)-\zeta(t)}\right), & s\neq t,\\ \dfrac{1}{\pi}\left(\dfrac{1}{2}\operatorname{Im}\dfrac{\zeta''(t)}{\zeta'(s)}-\operatorname{Im}\dfrac{\hat{A}(t)}{\hat{A}(s)}\right), & s=t.\end{cases}$$

The classical Neumann kernel is the generalized Neumann kernel formed with $\hat{A}(t)=1$, i.e.

$$N(t,s)=\frac{1}{\pi}\operatorname{Im}\left(\frac{\zeta'(s)}{\zeta(s)-\zeta(t)}\right)$$

The adjoint kernel $N^*(s,t)$ of the Neumann kernel is as follows:

$$N^*(t,s)=N(s,t)=\frac{1}{\pi}\operatorname{Im}\left(\frac{\zeta'(t)}{\zeta(t)-\zeta(s)}\right)$$

The generalized Neumann kernel $\tilde{N}(s,t)$ is as follows:

$$\tilde{N}(t,s)=\frac{1}{\pi}\operatorname{Im}\left(\frac{\tilde{A}(t)}{\tilde{A}(s)}\frac{\zeta'(s)}{\zeta(s)-\zeta(t)}\right),\tilde{A}(t)=\frac{\zeta'(t)}{\hat{A}(t)}$$

If $\hat{A}=1$, then

$\tilde{N}(t,s)=-N^*(t,s)$.

Refer to Sangawi [10] for the definitions of $N, \tilde{N}$ and N^*.

3. INTEGRAL EQUATION METHOD FOR COMPUTING THE FUNCTION $\mathcal{F}$

The canonical region can be described as a disk with a finite straight slit along the line where $\operatorname{Im}\mathcal{F}=0$, as well as M−1 finite spiral slits. Additionally, there is a rectilinear slit, which refers to a slit that lies on a straight line.

$$\operatorname{Im}\left[e^{-i\alpha}\mathcal{F}\right]=r,\quad \alpha,r\in\mathbb{R},$$

The variable α represents the angles of intersection between the line and the real axis. There is also a spiral slit, which refers to a slit that is located on a logarithmic spiral.

$$\operatorname{Im}\left[e^{-i\alpha}\log\mathcal{F}\right]=r,\quad \alpha,r\in\mathbb{R},$$

Where the oblique angles α are prescribed in advance.

Assume that the function $\mathcal{F}(\zeta)$ maps the curve Γ_0 onto the circle with radius e^{-R_0}, the circle Γ_1 onto a finite rectilinear slit that lies on the line where Im $(\mathcal{F}(\zeta))=0$, and the curves Γ_ι, where $\iota=2,\ldots,M$, onto $M-1$ finite spiral slits with oblique angles θ_ι, $\iota=2,\ldots,M$. Therefore, the mapping function that transforms Ω onto Ω_1 and Ω_2 fulfills the following conditions.

$$\left|\mathcal{F}(\zeta)\right|=e^{-R_0},\quad t\in I_0 \tag{1}$$

$$\operatorname{Im}\left(\log\left(\mathcal{F}\left(\zeta(t)\right)\right)\right)=0,\quad t\in I_1 \tag{2}$$

$$\operatorname{Im}\left(e^{-i\theta_\iota}\log\left(\mathcal{F}\left(\zeta_\iota(t)\right)\right)\right)=R_\iota,\quad t\in I_\iota,\ \iota=2,\ldots,M \tag{3}$$

The values $R_0,R_1,\ldots,R_M$ are real constants that have not been determined, $\theta(t)=(\pi/2,0,\theta_2,\ldots,\theta_M)$, $R(t)=(R_0,0,R_2,\ldots,R_M)$ [14]. Hence $\mathcal{F}(\zeta)$ satisfy

$$\operatorname{Re}\left(e^{i(0.5\pi-\theta_\iota)}\log\left(\mathcal{F}\left(\zeta_\iota(t)\right)\right)\right)=-R_\iota,\quad t\in I_\iota,\quad \iota=0,\ldots,M, \tag{4}$$

And $\mathcal{F}(\zeta)$ can be reformulated as [14]:

$$\frac{\mathcal{F}(\zeta)}{K_1(\zeta)}=K_2(\zeta)e^{(\zeta-\alpha)\hat{h}(\zeta)+ih_1}, \tag{5}$$

Where,

$$K_1(\zeta)=\begin{cases}\left(\dfrac{\zeta^2+p^2}{2p\zeta}\right)+c, & \zeta\in\Gamma_1,\\ 1, & \zeta\notin\Gamma_1,\end{cases}$$

$$K_2(\zeta)=\begin{cases}1, & \zeta\in\Gamma_1,\\ \left(\dfrac{\zeta^2+p^2}{2p\zeta}\right)+c, & \zeta\notin\Gamma_1,\end{cases}$$

ρ is a radius of Γ_1 c=1 for Ω_1, c=0 for Ω_2, $\hat{h}(\xi)$ is an analytic function in Ω_1 for $c=1$ and $\hat{h}(\xi)$ is an analytic function in Ω_2 for $c=0$. And then define $S(t)$ by,

$$\bar{B}\log\left(\frac{\mathcal{F}(\zeta)}{K_1(\zeta)}\right)=r(t)+iS(t),\ \bar{B}=e^{i(0.5\pi-\theta_\iota)},\quad r_\iota=-R_\iota,\ \iota=0,\ldots,M, \tag{6}$$

We assume that,

$$F(\zeta)=e^{\bar{B}\log\left(\frac{\mathcal{F}(\zeta)}{K_1(\zeta)}\right)}=e^{r_\iota+iS_\iota(t)},\quad \iota=0,\ldots,M, \tag{7}$$

which implies that,

$$F'(\zeta_\iota(t))\zeta'_\iota(t)=iS'_\iota(t)F(\zeta_\iota(t)),\quad j=0,\ldots,M. \tag{8}$$

After some algebraic manipulations, we obtain,

$$\overline{\left(\frac{F'(\zeta)}{F(\zeta)}\right)}=-T(\zeta)^2\left(\frac{F'(\zeta)}{F(\zeta)}\right),\ T(\zeta)=\left(\frac{\zeta'(t)}{\zeta(t)}\right),\zeta\in\Gamma. \tag{9}$$

From the definitions of $F(\zeta)$ and $\mathcal{F}(\zeta)$ we obtain,

$$F(\zeta)=e^{B\log(K_2(\zeta))}e^{\bar{B}((\zeta-\alpha)\hat{h}(\zeta)+ih_1)}, \tag{10}$$

Let,

$$D(\zeta)=\frac{BF'(\zeta)}{F(\zeta)}-\frac{k'_2(\zeta)}{k_2(\zeta)},\ \text{is analytic in } \Omega. \tag{11}$$

$$\frac{K'_2(\zeta)}{K_2(\zeta)}=\begin{cases}0, & Z\in\Gamma_1,\\ \left(\dfrac{\zeta^2-p^2}{\zeta(\zeta^2+2cp\zeta+p^2)}\right), & Z\notin\Gamma_1,\end{cases}$$

Combining (9) and (11), we obtain,

$$D(\zeta)=-\frac{B(\zeta)\overline{T(\zeta)}}{\overline{B(\zeta)}T(\zeta)}\overline{D(\zeta)}-B(\zeta)^2\,\overline{T(\zeta)}^2\overline{\left(\frac{k'_2(\zeta)}{k_2(\zeta)}\right)}-\frac{k'_2(\zeta)}{k_2(\zeta)},\ \zeta\in\Gamma \tag{12}$$

Equation (10), yields,

$$\log\left(F(\zeta(t))\right)=\bar{B}\log\left(K_2(\zeta(t))\right)+\bar{B}\left[(\zeta(t)-\alpha)\hat{h}(\zeta(t))+ih_1\right] \tag{13}$$

We reach the following from (7):

$$\log\left(F(\zeta(t))\right) = r_\iota + iS_\iota(t), \text{ where } r_\iota = -R_\iota, \quad \iota = 0,\ldots,M, \tag{14}$$

then

$$\bar{B}\left(\zeta(t)-\alpha\right)\hat{h}\left((t)\right) = r_j + h_1\cos\theta + i\left(\rho(t)+\hat{\upsilon}(t)-h_1\sin\theta\right) - \bar{B}\log\left(K_2\left(\zeta(t)\right)\right) = h(t) + i\left(\rho(t)+\upsilon(t)\right)+\gamma(t)+i\mu(t), \tag{15}$$

where

$\gamma(t)+i\mu(t) = -\bar{B}\log\left(K_2\left(\zeta(t)\right)\right)$, $h(t) = r_\iota + h_1\cos\theta$ and $\upsilon(t) = \hat{\upsilon}(t) - h_1\sin\theta$.

By obtaining h_ι, $\iota=0,\ldots,M$, from second equation in Theorem 2; Sangawi [11] we obtain

$$r_\iota = h_\iota - h_1\cos\theta_\iota, \quad \iota = 0,\ldots,M \tag{16}$$

By using Theorem 1 in Sangawi [11], (11), (12) and after some algebraic operations we achieve the following:

$$\frac{F'(\zeta)}{F(\zeta)}T(\zeta) + \frac{1}{\pi}\int_\Gamma \mathrm{Im}\left[\frac{\overline{B(\zeta)}}{\overline{B(w)}}\frac{T(\zeta)}{\zeta-\xi}\right]\frac{F'(\xi)}{F(\xi)} T(\xi)|d\xi| = 2i\,\mathrm{Im}\left[\frac{\overline{B(\zeta)}T(\zeta)K_2'(\zeta)}{K_2(\zeta)}\right], \zeta\in\Gamma \tag{17}$$

Assume that $\xi=\xi(t)$ and $\xi=\xi(s)$. Then by placing $F'(\zeta)\zeta'(t)\,/\,F(\zeta) = iS_\iota'(t)$, $\xi\in\Gamma$ in (17), we realize

$$S_\iota'(t) + \int_I \tilde{N}(s,t)S_\iota'(s)ds = 2\,\mathrm{Im}\left[\frac{\overline{B(\zeta)}\zeta'(t)K_2'(\zeta(t))}{K_2(\zeta(t))}\right],$$

this can be written in its operator form ($\tilde{N} = -N^*$)

$$\left(I+N^*\right)S_\iota' = 2\,\mathrm{Im}\left[\frac{\overline{B(\zeta)}\zeta'(t)K_2'(\zeta(t))}{K_2(\zeta(t))}\right] \tag{18}$$

As a result, (18) is not uniquely solvable. To deal with this problem, observe

$$\int_I S_\iota'(t)\,dt = 0, \quad \iota = 1,\ldots,M$$

which implies

$$JS_\iota' = 0 \tag{19}$$

The combination of (18) and (19) gives:

$$\left(I+N^*+J\right)S_\iota' = 2\,\mathrm{Im}\left[\frac{\overline{B(\zeta)}\zeta'(t)K_2'(\zeta(t))}{K_2(\zeta(t))}\right]. \tag{20}$$

In the light of [14, Theorem 2], (20) is uniquely solvable. $S_\iota'(t)$ gives the value of $S_\iota(t)$, $\iota = 0,\ldots,M$, by using the following equation.

$$S_\iota(t) = \int S_\iota'(t)dt + \upsilon_\iota =: \rho_\iota(t) + \upsilon_\iota, \quad t\in I_\iota, \tag{21}$$

where υ_ι is a real constant integration, we see that,

$$\rho_\iota(t) = \int S_\iota'(t)dt, \quad t\in I_\iota \tag{22}$$

h_ι is obtained through solving (13) and (11) in Sangawi [11] from which r_ι is provided through (16). Having solved (20) we are granted the value $S_\iota'(t)$. We obtain υ_ι through the equations (37), (38) and (12) in Sangawi [11] from which $\hat{\upsilon}_\iota$ is acquired, after that $\mathcal{F}(\zeta)$ is attained by,

$$\mathcal{F}\left(\zeta_\iota(t)\right) = K_1\left(\zeta_\iota(t)\right)e^{B(r_\iota + i(\rho_\iota(t)+\hat{\upsilon}_\iota(t)))}, \quad j = 0,\ldots,M. \tag{23}$$

Using the Cauchy integral formula, the interior value of $\mathcal{F}(\zeta)$ is determined.

4. NUMERICAL EXAMPLES

Nyström's method alongside the trapezoidal rule [17] [18] was used to solve (13) in Sangawi [11] and (20). The computational details are almost identical to [19], [20].

Some test regions of connectivity three, four, and seven have been used for numerical experiments [14]. MATLAB R2020a was used to carry out all the computations. In each boundary Γ_j the same number of collocation point has been used. Ω, Ω_1 and Ω_2 are shown in Figures 2-4. Tables 1-3 exhibit our computed values of r_ι, $\iota=0,\ldots,6$ compared to those of Nasser [14].

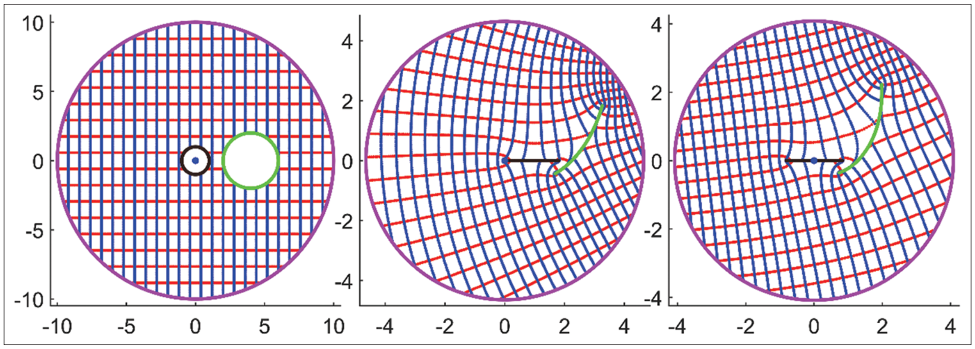

Fig. 2. Mapping Ω onto Ω_1 and Ω_2 with three connectivity.

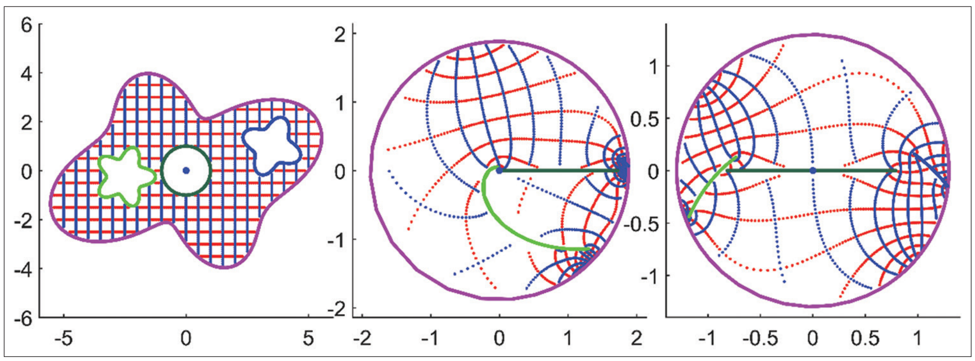

Fig. 3. Mapping Ω onto Ω_1 and Ω_2 with four connectivity.

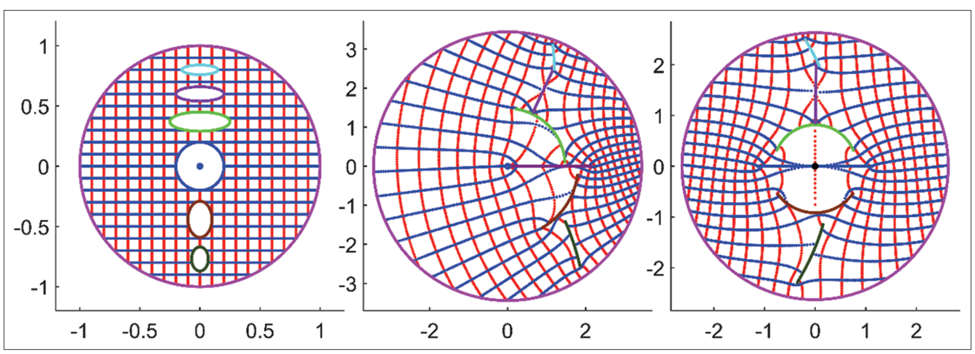

Fig. 4. Mapping Ω onto Ω_1 and Ω_2 with seven connectivity.

Example 1

The region with the following boundaries:

$$\Gamma_0 : \left\{\zeta(\mathrm{t}) = 10\left(\cos t + i \sin t\right)\right\},$$

$$\Gamma_1 : \left\{\zeta(\mathrm{t}) = \cos t - i \sin t\right\},$$

$$\Gamma_2 : \left\{\zeta(\mathrm{t}) = 4 + 2(\cos t - i \sin t)\right\},$$

$$\mathrm{t} \in [0, 2\text{À}], \quad = \left(\frac{\pi}{2}, 0, -\frac{3\pi}{4}\right), \quad \alpha = 2 + 3i$$

Table 1 give the computed values of r and Ω, Ω_1 and Ω_2 are shown in Figure 2.

Example 2

The region Ω bounded by four multiply connected region, Nasser [14],

$$\Gamma_0 : \left\{\zeta(t) = \left(4 + \cos 2t + \sin 4t\right) e^{it}\right\},$$

$$\Gamma_1 : \left\{\zeta(t) = e^{-it}\right\},$$

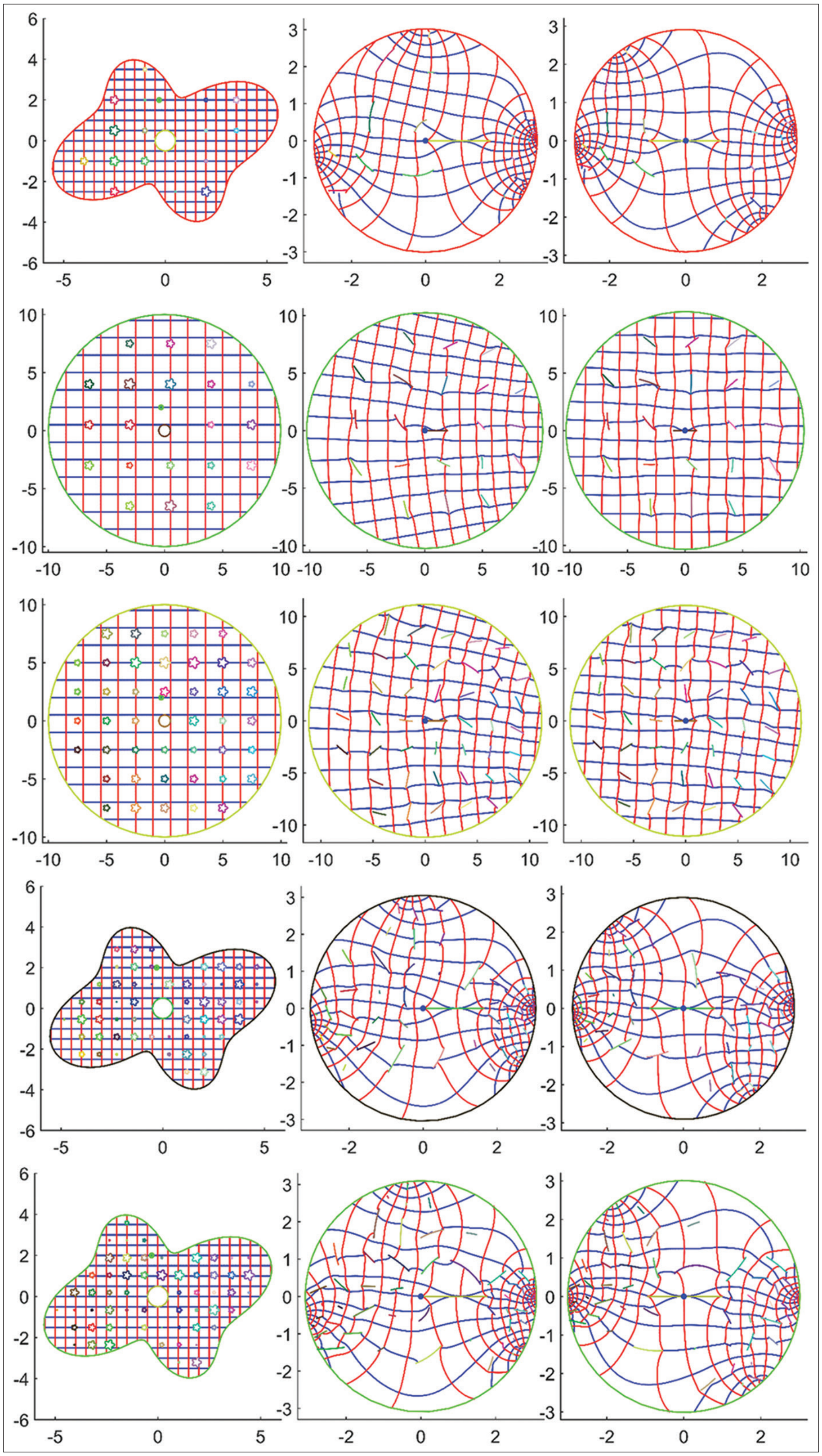

Fig. 5. Ω, Ω_1 and Ω_2 with high connectivity.

Table 1: Computed values of $r_\iota,\iota=0,1,2$

n	r_0	r_1	r_2
Computed values of $r_\iota,\iota=0,1,2$ for Ω_1			
32	1.53579417691881	0	−0.570199621240809
64	1.53579417442883	0	−0.570199620799919
128	1.53579417442883	0	−0.570199620799919
Computed values of $r_\iota,\iota=0,1,2$ for Ω_2			
32	1.40674522978284	0	−0.174539534772558
64	1.40674523035241	0	−0.174539535774301
128	1.40674523035241	0	−0.174539535774301

Table 2: Computed values of $r_\iota,\iota=0,\ldots,3$ with n=128

r_ι	Proposed method	Presented method in Nasser [11]
Computed values of $r_\iota,\iota=0,\ldots,3$ for Ω_1		
r_0	0.632297599993722	0.632297593480685
r_1	0	0
r_2	0.89615354957018	0.896153544382371
r_3	0.47224415769662	0.472244154231282
Computed values of $r_\iota,\iota=0,\ldots,3$ for Ω_2		
r_1	Proposed method	Presented method in Nasser [11]
r_0	0.260931620532661	0.260931605731473
r_1	0	0
r_2	2.13317552874793	2.13317551821617
r_3	0.100276605317663	0.100276596055608

Table 3: Computed values of $r_\iota,\iota=0,\ldots,6$

r_ι	Proposed method	Presented method in Nasser [11]
Computed values of $r_\iota,\iota=0,\ldots,6$ for Ω_1		
r_0	1.23570971232484	1.235709712326
r_1	0	0
r_2	0.390611187505815	0.390611187504613
r_3	−1.12990942307151	−1.12990942307163
r_4	−0.537364361903202	−0.537364361903388
r_5	0.590670832485013	0.590670832470072
r_6	−0.43049693297431	−0.430496932984193
Computed values of $r_\iota,\iota=0,\ldots,6$ for Ω_2		
r_ι	Proposed method	Presented method in Nasser [11]
r_0	0.967817156520659	0.967817156521745
r_1	0	0
r_2	−0.202389826842849	−0.202389826843975
r_3	−1.56125001631144	−1.56125001631162
r_4	−1.05242061198575	−1.05242061198594
r_5	−0.0844703418222131	−0.0844703418361004
r_6	−1.2703736171962	−1.27037361720976

$$\Gamma_2 \;:\left\{\zeta(t)=\left(1+0.25\cos 5t\right)e^{-it}\right\},$$

$$\Gamma_3 \;:\;\{\zeta(t)=(1+0.25\sin 4t)e^{-it},$$

$$t\in[0,2\pi],=\left(\frac{\pi}{2},0,\frac{\pi}{4},\frac{3\pi}{4}\right),\;\; \alpha=2i$$

The values of $r_\iota,\iota=0,\ldots,3$ are listed in Table 2 and Ω, Ω_1 and Ω_2 are shown in Figure 3.

Example 3

The region Ω bounded by seven multiply connected region, Nasser [11],

$$\Gamma_0 \;:\left\{\zeta(t)=e^{it}\right\},$$

$$\Gamma_1 \;:\left\{\zeta(t)=0.2e^{-it}\right\},$$

$$\Gamma_2 \;:\left\{\zeta(t)=i0.37+0.25\cos t-i0.08\sin t\right\},$$

$$\Gamma_3 \;:\left\{\zeta(t)=i0.6+0.2\cos t-i0.06\sin t\right\},$$

$$\Gamma_4 \;:\left\{\zeta(t)=i0.8+0.15\cos t-i0.04\sin t\right\},$$

$$\Gamma_5 \;:\left\{\zeta(t)=-i0.44+0.1\cos t-i0.15\sin t\right\},$$

$$\Gamma_6 \;:\left\{\zeta(t)=-i0.77+0.07\cos t-i0.1\sin t\right\},$$

$$t\in[0,2\text{À}],\quad \alpha=0.5+0.5i,$$

$$\theta=\left(0.5\pi,0,0.5\pi,0,0.15\pi,0.5\pi,0.875\pi\right)$$

The values of $r_\iota,\iota=0,\ldots,6$ are listed in Table 3 and **Ω, Ω_1 and Ω_2** are shown in Figure 4. Some more examples are shown in Fig. 5.

5. CONCLUSIONS

The present study proposes a new boundary integral equation for the conformal mapping of multiply connected regions onto the disk with rectilinear slit and spiral slits regions, Ω_1 and Ω_2. We used the proposed method to compute several mappings of some test regions and computed the boundary values of the mapping function. The interior mapping function was then determined using Cauchy's integral formula. Numerical examples were provided to demonstrate the high accuracy of the boundary integral equation method.

ACKNOWLEDGMENTS

This work was supported in part by the Ministry of Higher Education through the Charmo University, Kurdistan, Iraq.

This support is gratefully acknowledged. I wish to thank Prof. Dr. Arif Asraf for his cooperation and thank an anonymous referee for valuable comments and suggestions on the manuscript which improve the presentation of the paper.

REFERENCES

[1] P. Koebe. Abhandlungen zur Theorie der konfermen Abbildung. IV. Abbildung mehrfach zusammenhängender schlicter Bereiche auf Schlitzcereiche (in German), *Acta Mathematica,* vol. 41, no. 1916, pp. 305-344.

[2] M. M. S. Nasser and A. A. Al-Shihri Fayzah. “A fast boundary integral equation method for conformal mapping of multiply connected regions”. *SIAM Journal on Scientific Computing,* vol. 35, no. 3, pp. A1736-A1760, 2013.

[3] M. M. S. Nasser. “A boundary integral equation for conformal mapping of bounded multiply connected regions”. *Computational Methods and Function Theory*, vol. 9, no. 1, pp. 127-143, 2009.

[4] M. M. S. Nasser. “Numerical conformal mapping via boundary integral equation with the generalized Neumann kernel”. *SIAM Journal on Scientific Computing*, vol. 31, pp. 1695-1715, 2009.

[5] M. M. S. Nasser. “Numerical conformal mapping of multiply connected regions onto the second, third and fourth categories of Koebe’s canonical slit domains”. *Journal of Mathematical Analysis and Applications*, vol. 382, pp. 47-56, 2011.

[6] M. M. S. Nasser, A. H. M. Murid and A. W. K. Sangawi. “Numerical conformal mapping via a boundary integral equation with the adjoint generalized Neumann kernel”. *TWMS Journal of Pure and Applied Mathematics*, vol. 5, no. 1, pp. 96-117, 2014.

[7] Z. Nehari. “*Conformal Mapping”*. Dover Publication, New York, 1952.

[8] A. W. K. Sangawi, A. H. M. Murid and M. M. S. Nasser. “Linear integral equations for conformal mapping of bounded multiply connected regions onto a disk with circular slits”. *Applied Mathematics and Computation,* vol. 218, no. 5, pp. 2055-2068, 2011.

[9] A. W. K. Sangawi and A. H. M. Murid. “Annulus with spiral slits map and its inverse of bounded multiply connected regions”. *International Journal of Scientific Engineering and Research*, vol. 4, no. 10, pp. 1447-1454, 2013.

[10] A. W. K. Sangawi. “Spiral slits map and its inverse of bounded multiply connected regions”. *Applied Mathematics and Computation,* vol. 228, pp. 520-530, 2014.

[11] A. W. K. Sangawi. “Straight slits map and its inverse of bounded multiply connected regions”. *Advances in Computational Mathematics*, vol. 41, pp. 439-455, 2015.

[12] A. W. K. Sangawi, A. H. M. Murid and L. Khiy. “Fast computing of conformal mapping and its inverse of bounded multiply connected regions onto second, third and fourth categories of Koebe’s canonical slit regions”. *Journal of Scientific Computing,* vol. 68, pp. 1124-1141, 2016.

[13] G. C. Wen. “*Conformal Mapping and Boundary Value Problems.* English Translation of Chinese Edition, 1984. American mathematical Society, Providence, 1992.

[14] M. M. S. Nasser. “Numerical conformal mapping of multiply connected regions onto the fifth category of Koebe’s canonical slit regions”. *Journal of Mathematical Analysis and Applications*, vol. 398, pp. 729-743, 2013.

[15] T. K. DeLillo, T. A. Driscoll, A. R. Elcrat and J. A. Pfaltzgraff. “Radial and circular slit maps of unbounded multiply connected circle domains”. *Proceedings: Mathematical, Physical and Engineering Sciences*, vol. 464, no. 2095, pp. 1719-1737, 2008.

[16] R. Wegmann and M. M. S. Nasser. “The Riemann-Hilbert problem and the generalized Neumann kernel on multiply connected regions”. *Journal of Computational and Applied Mathematics*, vol. 214, pp. 36-57, 2008.

[17] K. E. Atkinson. “*The Numerical Solution of Integral Equations of the Second Kind*”. Cambridge University Press, Cambridge, 1997.

[18] P. J. Davis and P. Rabinowitz. “*Methods of Numerical Integration*”. 2nd ed. Academic Press, Orlando, 1984.

[19] A. H. M. Murid and H. Laey-Nee. “Numerical experiment on conformal mapping of doubly connected regions onto a disk with a slit”. *International Journal of Pure and Applied Mathematics*, vol. 51, no. 4, pp. 589-608, 2009.

[20] A. H. M. Murid and H. Laey-Nee. “Numerical conformal mapping of bounded multiply connected regions by an integral equation method”. *International Journal of Contemporary Mathematical Sciences,* vol. 4, no. 23, pp. 1121-1147, 2009.